Chinese Chemical Letters 32 (2021) 150–153

Contents lists available at ScienceDirect

Chinese Chemical Letters

journal homepage: www.elsevier.com/locate/cclet

Communication

Synthesis of highly ordered AgNPs-coated silica photonic crystal beads for sensitive and reproducible 3D SERS substrates

Juan Li[a,**], Wanling Li[a], Yan Rao[a], Feng Shi[a], Suhua Yu[b], Huizhen Yang[a], Lingfeng Min[c,**], Zhanjun Yang[a,b,*]

[a] School of Chemistry and Chemical Engineering, Yangzhou University, Yangzhou 225002, China
[b] Guangling College, Yangzhou University, Yangzhou 225002, China
[c] Department of Laboratory Medicine and Clinical Medical College of Yangzhou University, Yangzhou 225001, China

ARTICLE INFO

Article history:
Received 14 August 2020
Received in revised form 16 September 2020
Accepted 28 October 2020
Available online 29 October 2020

Keywords:
Surface enhanced Raman scattering
Photonic crystal
3D ordered substrate
Silver nanoparticles
Malachite green

ABSTRACT

3D highly ordered silver nanoparticles (AgNPs) coated silica photonic crystal beads (Ag/SPCBs) were prepared and exploited as a novel surface enhanced Raman scattering (SERS) substrate. The monodisperse and size-controlled SPCBs were prepared *via* self-assembly of silica nanoparticles process using a simple microfluidic device. Then the Ag/SPCBs were easily obtained by *in situ* growth of AgNPs onto the NH_2-modified SPCBs. Field emitting scanning electron microscopy (SEM) and energy dispersive X-ray spectrometry (EDX) were used to characterize the Ag/SPCBs. The effect of silica nanoparticle size and $AgNO_3$ concentration on the SERS performance of the resultant Ag/SPCBs substrate were discussed in detail. The results indicate that the Ag/SPCBs have highest SERS signals when silica nanoparticle size is 250 nm and $AgNO_3$ concentration is 0.8 mg/mL. Using malachite green (MG) as model analyte, the Ag/SPCBs substrate displayed a high sensitivity and a wide linear range for MG. The well-designed Ag/SPCBs show high uniformity and excellent reproducibility, and can be used as an effective SERS substrate for sensitive assay application.

Surface enhanced Raman scattering (SERS) techniques have been considered as one very promising tool for molecular analysis because of its unique narrow band, high sensitivity, and non-destruction [1–4]. Nowadays SERS detection has been widely exploited in various fields [5,6]. However, there are still some problems such as unfavorable activity and stability presented in the SERS substrates [5,7]. Recent researches have indicated that ideal SERS substrates have considerable amount of nano-scaled gaps (or hotspots) for high sensitivity in the SERS analysis as well as a large specific surface area to adsorb lots of analytes. The hierarchical metallic structures have been extensively used as SERS substrates [8–10] due to excellent properties. These types of SERS substrates were mostly prepared by employing approaches or by producing plasmonic nanoparticles with core-shell structures. In compassion with two dimensional SERS substrates, three dimensional (3D) hierarchical metallic structured substrates can enable a large surface specific area with an abundant hotspots [11,12]. Unfortunately, it is very hard to obtain stable and reproducible 3D hierarchical metallic structures.

Photonic crystal beads (PCBs), which compose with periodically arranged monodisperse nanoparticles, show a number of important advantages in fabricating SERS substrates because of highly uniform structure and excellent stable and reproducibility [13–15]. The silica photonic crystal beads (SPCBs) as one of many 3D ordered structure templates have the advantages such as good stability, easy preparation and a huge specific surface area for the metal particles growth [16]. However, it is still a great challenge for metal nanoparticles to grow uniformly and form a considerable amount of hot spots on the surface of SPCBs.

Malachite green (MG) is a well-known organic compound, and has been widely used as dyestuff in the leather, ceramics, paper and food industries [17]. However, previous studies have shown that MG is teratogenic, carcinogenic and mutagenic for both humans and animals [18]. Hence, monitoring and detecting MG in environmental samples has become very important. Up to now many assay methods, including high-performance liquid chromatography [19], spray-mass spectrometric [20], liquid

* Corresponding author at: School of Chemistry and Chemical Engineering, Yangzhou University, Yangzhou 225002, China.
** Corresponding authors.
E-mail addresses: lijuan@yzu.edu.cn (J. Li), minlingfeng@126.com (L. Min), zjyang@yzu.edu.cn (Z. Yang).

https://doi.org/10.1016/j.cclet.2020.10.043
1001-8417/

chromatography–tandem mass spectrometry [21] and fluorescent sensor [22], have been reported for detection of MG. But above-mentioned methods rely on expensive facilities and complex sample pretreatment process. Thus it is urgently needed to explore an efficient assay method for simple and sensitive detection of MG.

Herein, Ag nanoparticles coated silica photonic crystal beads (Ag/SPCBs) were fabricated as SERS substrates for MG detection. Monodisperse size-controlled SPCBs were firstly prepared through self-assembly of silica nanoparticles by a microfluidic device, and then AgNPs were *in situ* deposited onto these NH_2-modified SPCBs (Scheme 1). The effect of silica nanoparticles size and $AgNO_3$ concentration on the SERS detection of the Ag/SPCBs were examined. The morphology of Ag/SPCBs was investigated by scanning electron microscopy (SEM). The prepared Ag/SPCBs were used as the novel SERS substrates for sensitive detection of MG. This 3D stable and reproducible SERS substrate presented a promising platform for ultrasensitive MG measurements.

Three kinds of SPCBs were synthesized by different size of the silica nanoparticles and recorded as SPCBs I, SPCBs II and SPCBs III, respectively. It can be observed from SEM images of Fig. 1, these SPCBs were arranged in a hexagonal close-packed structure. And the sizes of the silica nanoparticles which form the three kinds of SPCBs are about 210 nm (Fig. 1A), 240 nm (Fig. 1B) and 280 nm (Fig. 1C), respectively. The inset SEM images of Fig. 1 shows that all the SPCBs are spherically shaped structure with a smooth edge, and show a uniform size of about 350 μm.

The resultant SPCBs were treated with piranha solution, and modified with the NH_2 group on the surface. After that, AgNPs were deposited onto the SPCBs by *in situ* reduction of $AgNO_3$. Using the SPCBs II as the model substrate, the effect of $AgNO_3$ concentration on the structure and morphology of the Ag/SPCBs was investigated. Fig. 2 shows the SEM images of Ag/SPCBs II which were obtained at $AgNO_3$ concentration of 0.6, 0.8, 1.0, 1.2 and 1.4 mg/mL, respectively. When the $AgNO_3$ concentration was relatively low (0.6 mg/mL), the AgNPs were mainly grown around the SiO_2 nanoparticles (Fig. 2A). When the $AgNO_3$ concentration was 0.8 mg/mL, the AgNPs not only grew around the SiO_2 nanoparticles, but also showed a uniform distribution on the surface of SiO_2 nanoparticles (Fig. 2B). With the increase of $AgNO_3$ concentration, it was found that the oversized AgNPs were formed on the surface of SPCBs II (Figs. 2C and D). These oversized AgNPs even covered the original hexagonal close-packed structure of SPCBs (Fig. 2E), and showed irregular and chaotic morphology and size distribution. Fig. 2F showed the energy dispersive X-ray spectrometry (EDX) of Ag/SPCBs II with the different $AgNO_3$ concentration. The weight percent of Ag increased with the increase of $AgNO_3$ concentration and reached a maximum value when the $AgNO_3$ concentration is 1.2 mg/mL. Then weight percent of Ag decreased with the further increase of $AgNO_3$ concentration, which is due to the AgNPs falling off the SPCBs. In addition, the Ag/SPCBs I and Ag/SPCBs III were also prepared by *in situ* reduction of different concentrations of $AgNO_3$ and their SEM images and EDX spectra were shown in the Figs. S1 and S2 (Supporting information). Compared with the Ag/SPCBs II, the Ag/SPCBs I and Ag/SPCBs III displayed the similar nanostructure when the $AgNO_3$ concentration was changed gradually.

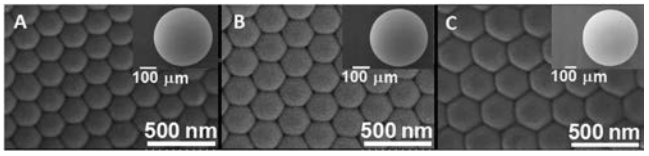

Fig. 1. SEM images of SPCBs I (A), SPCBs II (B), SPCBs III (C) and their magnifications, the size of SPCBs is about 350 μm.

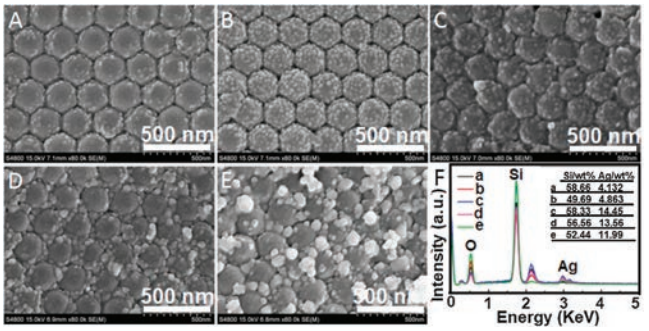

Fig. 2. SEM images (A-E) and EDX spectra (F) of Ag/SPCBs II obtained by *in situ* reduction of $AgNO_3$ at concentrations of (a-e) 0.6, 0.8, 1.0, 1.2 and 1.4 mg/mL.

Fig. 3 shows the 4-mercaptobenzoic acid (4-MBA, 0.02 mol/L) SERS spectra obtained from the Ag/SPCBs I (Fig. 3A), Ag/SPCBs II (Fig. 3C), and Ag/SPCBs III (Fig. 3E) treated in different concentration of $AgNO_3$. The Raman peaks of 4-MBA agreed well with literature data [21]. It can be found that the SERS intensities of 4-MBA molecules arrived at the highest values when Ag/SPCBs I, II and III were prepared at the $AgNO_3$ concentration of 0.8 mg/mL (Figs. 3B, D and F). When the concentrations of $AgNO_3$ is 0.6 mg/mL, the size and density of AgNPs on the surface of the Ag/SPCBs is relatively low, which gives the weakest SERS signal enhancement. With the increasing of $AgNO_3$ concentrations, the amount and density of AgNPs on the surface of the Ag/SPCBs increased gradually. At the same time, Ag nanoparticles began to get closer each other. The actions formed plasma coupling effect to produce a large number of hot spots, thus strongly enhancing the Raman signals. However, oversized AgNPs were formed on the surface of SPCBs after the concentration of $AgNO_3$ was beyond 0.8 mg/mL, which leaded to poor SERS enhancement due to the limited hot spots. Therefore, Ag/SPCBs obtained at $AgNO_3$ concentration of 0.8 mg/mL were optimal SERS substrate for molecules detection.

Moreover, SERS behavior of 4-MBA adsorbed on Ag/SPCBs I, Ag/SPCBs II and Ag/SPCBs III (being prepared at 0.8 mg/mL $AgNO_3$) were examined. As shown from Fig. S3 (Supporting information), SERS intensity values of 4-MBA on three types of Ag/SPCBs are close to each other, and Ag/SPCBs II shows a little stronger SERS enhancement compared with other two Ag/SPCBs substrates. The results demonstrate that silica nanoparticle sizes have small effect on the SERS enhancement of Ag/SPCBs. Thus, three kinds of Ag/SPCBs can be used for the quantitative SERS detection.

Under the selected conditions, three kinds of Ag/SPCBs were used for the quantitative detection of MG. SERS spectra of Ag/SPCBs I (Fig. 4A), Ag/SPCBs II (Fig. 4C), and Ag/SPCB III (Fig. 4E) for detection of different concentration of MG were displayed in Fig. 4. Three wide detection ranges from 1.0×10^{-12} to 1.0×10^{-7} g/mL, 1.0×10^{-13} to 1.0×10^{-7} g/mL and 1.0×10^{-12} to 1.0×10^{-7} g/mL for MG were obtained with Ag/SPCBs I (Fig. 4B), Ag/SPCBs II (Fig. 4D), and Ag/SPCB III (Fig. 4F) SERS enhancement substrates,

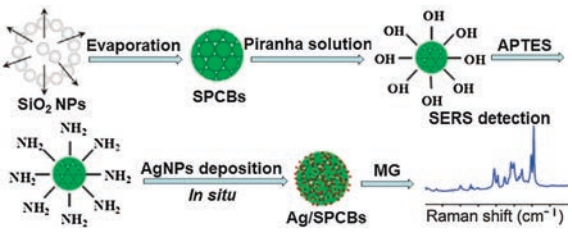

Scheme 1. The schematic diagram of the process for synthesis of Ag/SPCBs and SERS detection of MG.

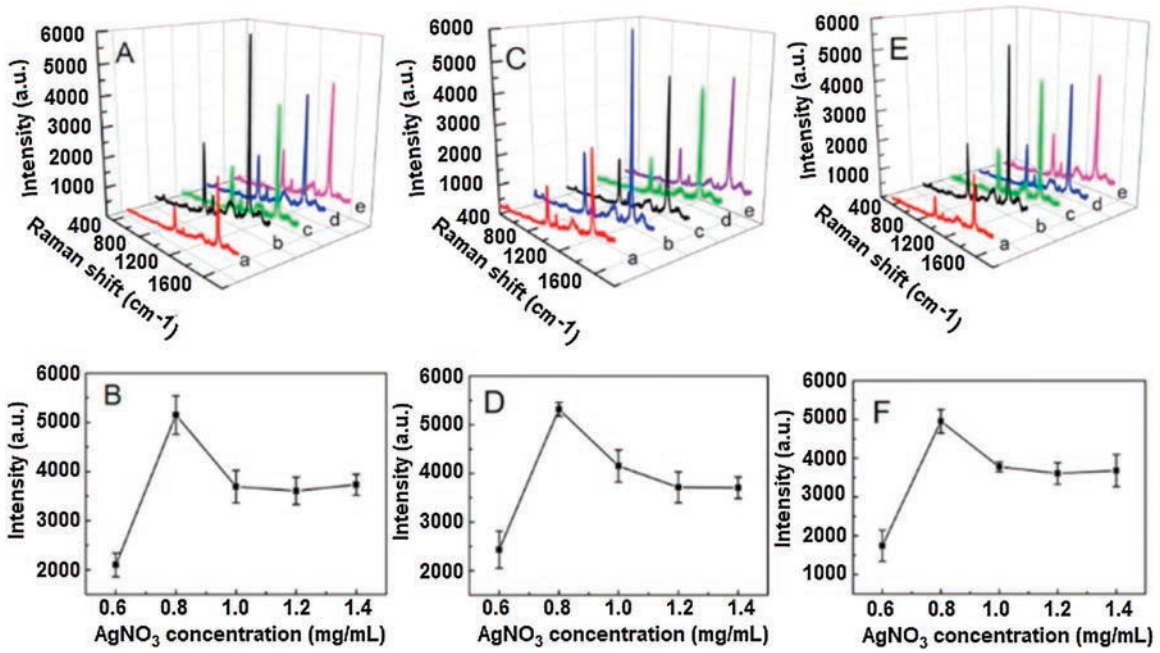

Fig. 3. SERS spectra of 4-MBA adsorbed on Ag/SPCBs I (A), Ag/SPCBs II (C) and Ag/SPCBs III (E), which were obtained by different concentrations of $AgNO_3$ (a-e: 0.6, 0.8, 1.0, 1.2 and 1.4 mg/mL, respectively). The normalized SERS intensity of 4-MBA adsorbed on Ag/SPCBs I (B), Ag/SPCBs II (D) and Ag/SPCBs III (F) with different $AgNO_3$ concentration at 1580 cm^{-1}.

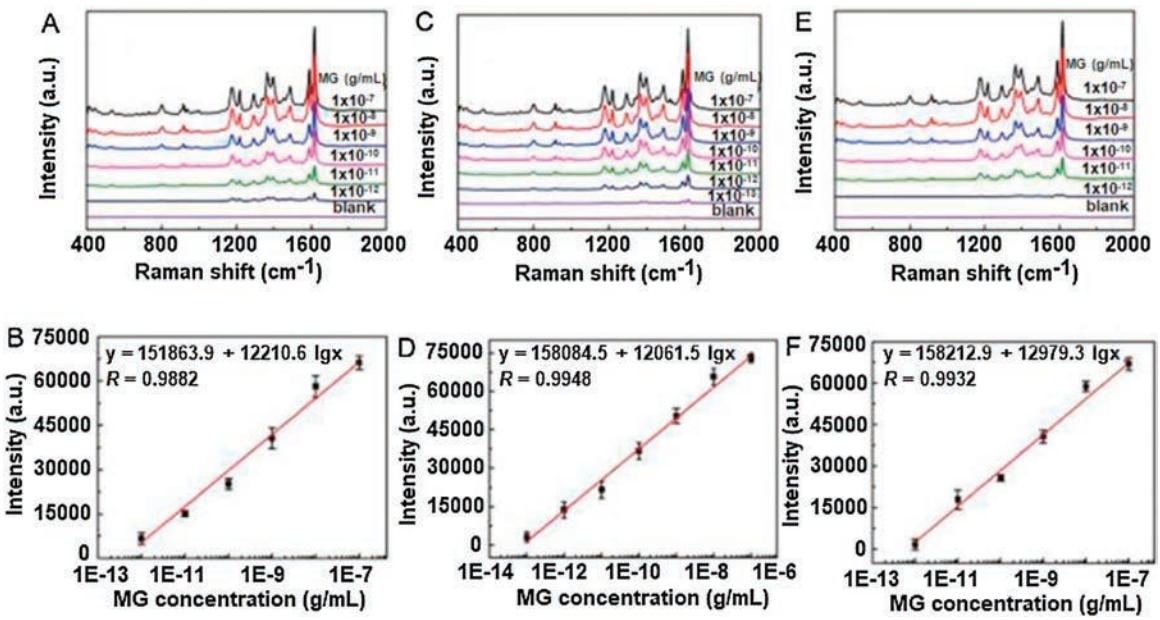

Fig. 4. SERS spectra of Ag/SPCBs I (A), Ag/SPCBs II (C), and Ag/SPCB III (E) for detection of different concentrations of MG. Calibration curves of MG at 1617 cm^{-1} with different SERS substrates: Ag/SPCBs I (B), Ag/SPCBs II (D), and Ag/SPCB III (F).

respectively. The detection limits for MG with three types Ag/SPCBs substrates were calculated to be 1.51×10^{-13}, 3.86×10^{-14} and 1.63×10^{-13} g/mL at a signal-to-noise (S/N) ratio of 3. It was found that sensitivity and linear range of Ag/SPCBs II in the detection of MG was better than other two types of substrates, which was consistent with the above-mentioned experimental results. Ag/SPCBs substrates show much lower detection limits of MG compared with previously reported SERS substrates [23–26]. Using Ag/SPCBs II as model, the intra- and inter-assay coefficients of variation (CVs) were examined. The intra-assay CV was the relative standard deviation (RSD) for five detections of MG on same-batch Ag/SPCBs substrate, and inter-assay CV was the RSD of five detections of MG on five-batch Ag/SPCBs substrates. The intra- and inter-assay CVs were calculated to be 3.3% and 5.7% at 1.0×10^{-10} g/mL of MG, respectively, suggesting satisfactory reproducibility for detection and fabrication of the Ag/SPCBs SERS substrates. After storing Ag/SPCBs substrate for one month at room temperature, no obvious SERS changes were observed, indicating the excellent stability of Ag/SPCBs substrate. The excellent performance of the Ag/SPCBs SERS substrates can be ascribed to the highly ordered and uniform structure, large specific surface area and large amounts of hot spots.

In this work, the SPCBs with good sphericity and the arrangement of internal particles were firstly fabricated by the microfluidic method and then were functionalized with NH_2 groups. The growth of AgNPs on NH_2-modified SPCBs were performed by *in situ* reduction of $AgNO_3$ process. The morphology and constitute of Ag/SPCBs were characterized with SEM and EDX. It was found that the concentration of $AgNO_3$ could greatly affect the morphology and size of AgNPs grown onto Ag/SPCBs. Ag/SPCBs obtained by the optimal $AgNO_3$ (0.8 mg/mL) can produce a large amount of hot spot, thus showing the largest SERS enhancement. Different size of SiO_2 nanoparticles for Ag/SPCBs provided the satiable surface area for AgNPs growth, and had no obvious the effect on the SERS enhancement. Three types of Ag/SPCBs I, II and III substrates were used for quantitative detection of malachite green, showing high assay sensitivity, very wide linear range and excellent reproducibility. The proposed Ag/SPCBs offered a novel and promising substrate for sensitive SERS assay application.

Declaration of competing interest

The authors report no declarations of interest.

Acknowledgments

The research received the financial support from National Natural Science Foundation of China (Nos. 21575125, 81870033 and 21475116), 333 Project and Qinglan Project of Jiangsu Province, Natural Science Foundation of Jiangsu Province (No. BK20191434), Six Talent Peaks Project of Jiangsu Province for Zhanjun Yang and Juan Li, High-end Talent Support Program of Yangzhou University for Zhanjun Yang and Juan Li, Priority Academic Program Development of Jiangsu Higher Education Institution (PAPD), Project for Science and Technology of Yangzhou (No. YZ2020068) and Open Research Fund of State Key Laboratory of Analytical Chemistry for Life Science (No. SKLACLS1915).

Appendix A. Supplementary data

Supplementary material related to this article can be found, in the online version, at doi:https://doi.org/10.1016/j.cclet.2020.10.043.

References

[1] H.K. Lee, Y.H. Lee, C.S.L. Koh, et al., Chem. Soc. Rev. 48 (2019) 731–756.
[2] Z.Y. Wang, S.F. Zong, L. Wu, et al., Chem. Rev. 117 (2017) 7910–7963.
[3] G.C. Phan-Quang, E.H.Z. Wee, F.L. Yang, et al., Angew. Chem. Int. Ed. 56 (2017) 5565–5569.
[4] J. Langer, D.J. de Aberasturi, J. Aizpurua, et al., ACS Nano 14 (2020) 28–117.
[5] S.R. Panikkanvalappil, S.M. Hira, M.A. Mahmoud, et al., J. Am. Chem. Soc. 136 (2014) 15961–15968.
[6] J.N. Zhang, P. Joshi, Y. Zhou, et al., Chem. Commun. 51 (2015) 15284–15286.
[7] H.L. Liu, Z.L. Yang, L.Y. Meng, et al., J. Am. Chem. Soc. 136 (2014) 5332–5341.
[8] Y.W. Qian, G.W. Meng, Q. Huang, et al., Nanoscale 6 (2014) 4781–4788.
[9] Y.W. Tan, J.J. Gu, L.H. Xu, et al., Adv. Funct. Mater. 22 (2012) 1578–1585.
[10] C. Huang, F.F. Lu, K. Xu, et al., Chin. Chem. Lett. 30 (2019) 2009–2012.
[11] S.Y. Lee, S.H. Kim, M.P. Kim, et al., Chem. Mater. 25 (2013) 2421–2426.
[12] S.Y. Cui, Z.G. Dai, Q.Y. Tian, et al., J. Mater. Chem. C 4 (2016) 6371–6379.
[13] Y.J. Zhao, L.R. Shang, Y. Cheng, et al., Acc. Chem. Res. 47 (2014) 3632–3642.
[14] M.S. Wang, L. He, W.J. Xu, et al., Angew. Chem. Int. Ed. 54 (2015) 7077–7081.
[15] C.X. Luan, H. Wang, Q. Han, et al., ACS Appl. Mater. Interfaces 10 (2018) 21206–21212.
[16] J. Li, S.J. Dong, J.J. Tong, et al., Chem. Commun. 52 (2016) 284–287.
[17] M. Yang, J. Yu, F. Lei, et al., Sens. Actuators B-Chem. 256 (2018) 268–275.
[18] P. Kumar, R. Khosla, M. Soni, et al., Sens. Actuators B-Chem. 246 (2017) 477–486.
[19] L.L. Zhang, Y.Y. Zhang, Y.R. Tang, et al., Int. J. Environ. Anal. Chem. 98 (2018) 215–228.
[20] S.C. Wei, S. Fan, C.W. Lien, et al., Anal. Chim. Acta 1003 (2018) 42–48.
[21] Y. Qin, J. Zhang, Y. Li, et al., Anal. Bioanal. Chem. 408 (2016) 5801–5809.
[22] W.Y. Gui, H. Wang, Y. Liu, et al., Sens. Actuators B-Chem. 266 (2018) 685–691.
[23] J. Zhao, C. Wu, L.P. Zhai, et al., J. Mater. Chem. C 7 (2019) 8432–8441.
[24] M. Shariati-Rad, N. Haghparast, Anal. Bioanal. Chem. 7 (2020) 131–150.
[25] X.H. Zhao, Z. Li, Y.F. Hao, et al., Spectrosc. Lett. 53 (2019) 63–75.
[26] Y. Zhao, Y.Y. Song, Y.Y. Zhang, et al., J. Food Meas. Charact. 14 (2019) 658–667.